

https://doi.org/10.1070/QEL16930

Optical properties of laser-modified diamond: From visible to microwave range

M.S. Komlenok, S.G. Tikhodeev, A.A. Khomich, S.P. Lebedev, G.A. Komandin, V.I. Konov

Abstract. **We have measured the optical properties of a graphitised layer with dc conductivity of 305 Ω^{-1} cm^{-1} produced by excimer laser irradiation (KrF, τ = 20 ns, λ = 248 nm) of a polycrystalline diamond surface grown by chemical vapour deposition. Studies have been conducted in a wide range of wavelengths: from far-IR to visible spectral regions. The resulting constants of the Drude model are the basic parameters for calculating the electromagnetic response of diamond/graphite photon elements or metamaterials fabricated using the direct laser writing method.**

Keywords: *laser, spectroscopy, optical properties, metamaterials, diamond, nanocrystalline graphite.*

1. Introduction

Laser graphitisation of the diamond surface and volume is an important task and is necessary in the manufacture of new elements of photonics and electronics [1–4]. Interest in this problem is primarily due to the very different electrical and optical properties of diamond and graphitised materials [5–7], formed as a result of a local laser-induced phase transition [8, 9]. This makes it possible to manufacture new photon elements using direct laser writing [10]. For example, this method can be used to produce three-dimensional photonic crystals [11, 12] or planar metamaterials [13]. To calculate the optical properties of fabricated structures, it is necessary to know their geometric characteristics and dielectric susceptibility of all the components of the structure of the materials. The optical properties of diamond are well studied in a wide spectral range [14]. At the same time, the electromagnetic response of a diamond graphitised by laser irradiation is unknown. This paper presents the experimental transmission spectra, as well as the calculated spectra of the dielectric response of the surface graphitised layer, obtained by fitting the calculated spectra to the experimental data, in the range from the far-IR region to the visible one.

M.S. Komlenok, V.I. Konov Prokhorov General Physics Institute, Russian Academy of Sciences, ul. Vavilova 38, 119991 Moscow, Russia; National Research Nuclear University 'MEPhI', Kashirskoe shosse 31, 115409 Moscow, Russia;
e-mail: komlenok@nsc.gpi.ru;
S.G. Tikhodeev Prokhorov General Physics Institute, Russian Academy of Sciences, ul. Vavilova 38, 119991 Moscow, Russia; M.V. Lomonosov Moscow State University, Vorob'evy gory, 119991 Moscow, Russia;
A.A. Khomich Prokhorov General Physics Institute, Russian Academy of Sciences, ul. Vavilova 38, 119991 Moscow, Russia; Kotelnikov Institute of Radioengineering and Electronics (Fryazino Branch), Russian Academy of Sciences, pl. Akad. Vvedenskogo 1, 141190 Fryazino, Moscow region, Russia;
S.P. Lebedev, G.A. Komandin Prokhorov General Physics Institute, Russian Academy of Sciences, ul. Vavilova 38, 119991 Moscow, Russia

Received 6 December 2018; revision received 15 February 2019
Kvantovaya Elektronika **49** (7) 672–675 (2019)
Translated by I.A. Ulitkin

2. Experiment

The substrate was a polished plate of polycrystalline diamond grown in a plasma microwave reactor using chemical vapour deposition. The plate had a thickness $d = 580 \pm 2$ μm and an area of 1 cm^2. The diamond surface was graphitised using an excimer KrF laser (Optosystems Ltd., CL 7100; λ = 248 nm, τ = 20 ns, pulse repetition rate f = 50 Hz) in a projection irradiation scheme, which made it possible to obtain a spot on the surface, whose shape and size is determined by the mask used [15]. A uniform graphitised layer was formed on the diamond surface using a square spot with a side of 200 μm. The sample was fixed on a translation stage and moved at a constant velocity, providing a specified number of pulses per point, i.e. four. The optical transmission spectra were measured in the frequency range of 30–1000 cm^{-1} using a Bruker IFS113v Fourier infrared spectrometer and a Specord M400 spectrometer working in the visible range.

3. Results and discussion

The diamond surface area measuring 4 × 4 mm was graphitised by the excimer laser radiation at an energy fluence of 35 J cm^{-2}. The thickness of the formed graphitised layer varied from 380 to 580 nm [16] depending on the orientation of the diamond crystallite on which graphitisation occured. The best agreement between the results of modelling the optical properties and experimental transmission spectra in the range of 30–40 cm^{-1} was obtained for a maximum thickness of 580 nm [17]. Therefore, we will use this value to simulate the electromagnetic response in the entire frequency range from 30 to 1000 cm^{-1}.

The transmission spectra of a diamond sample with a graphitised surface are shown in Fig. 1. Figure 1a compares the transmission spectra, measured in a wide frequency range – from 20 to 1.4×10^4 cm^{-1} ($\hbar\omega$ = 2.48 meV–1.74 eV or λ = 500–0.7 μm), with model spectra (green dashed line), calculated by the method described below. Figure 1b shows the low frequency range of 30–40 cm^{-1}. For this range, accurate calibration experimental data were obtained using an 'Epsilon' monochromatic spectrometer and a backward wave oscillator [18].

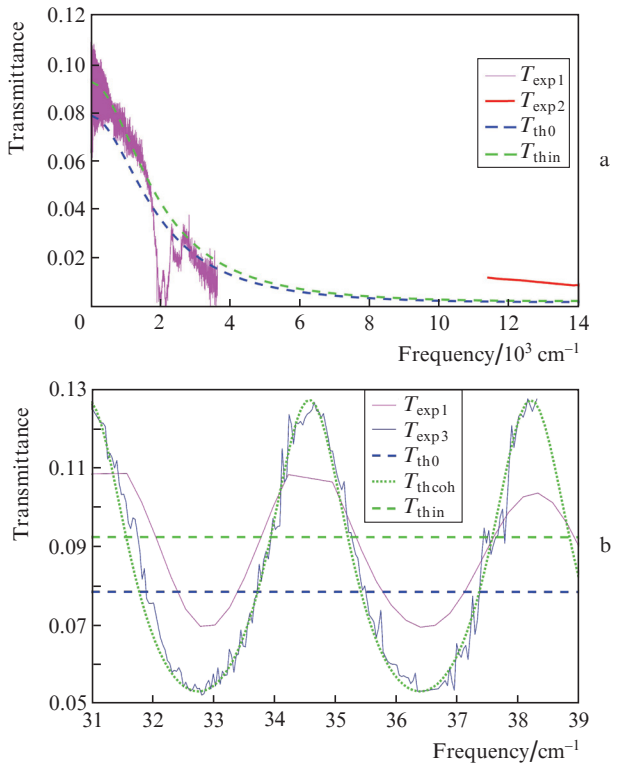

Figure 1. (Colour online) Experimental (solid curves) and calculated (dashed and dotted curves) transmittance spectra of a graphitised layer with $\varepsilon_\infty = 1$ (a) in a wide frequency range and (b) at a low-frequency edge. The green dashed line in Fig. 1b corresponds to fully coherent plane waves, green dotted curves were obtained in simulations neglecting interference effects, and blue dashed lines were obtained without taking into account multiple reflections in the diamond plate.

Optical transmission spectra of a diamond plate with a uniform graphitised layer on the upper surface, taking into account multiple reflections, can be calculated using any matrix method (see, for example, [19]). It should be noted that the boundary between the diamond and the graphitised layer may not be sufficiently sharp, which indicates the presence of a transition layer [20]. The layer graphitised as a result of laser irradiation is a mixture of nanocrystalline graphite and amorphous carbon [21, 22]. However, the observed inhomogeneities are of submicron size, and therefore the complete electromagnetic response of the medium allows description through the effective permittivity, for which it is correct to apply the Fresnel formula to calculate the reflection. We used an optical scattering matrix [23], which, in this case, reduces to a simple (2×2) transfer matrix.

In simulating the transmission spectra, the thickness of the diamond plate and the graphitised layer were assumed equal to 578 μm and 580 nm, respectively. The best value of the diamond permittivity ε_d was 5.6454 + 0.0001i, which corresponds to the refractive index $n_d + i\kappa_d = 2.376 + 2 \times 10^{-5}$i. The dispersion of the refractive index in the considered range is insignificant – the deviation from the reduced value does not exceed 0.01 [24, 25]; therefore, we did not take it into account in our calculations. A small attenuation in diamond ($\kappa_d = 2 \times 10^{-5}$) ensures good agreement between the calculated transmittance spectrum of the diamond plate (before graphitisation) and the experimental value in the visible range and agrees with the data for polycrystalline diamond [24]. In the experimental spectrum in the region of ~2000 cm^{-1}, two-phonon absorption is observed in diamond [14], which was not taken into account in modelling so that not to increase the number of fitting parameters (this absorption can, in principle, be taken into account by adding the corresponding Lorentz–Drude pole to the expression for ε_d) .

To calculate the permittivity of the graphitised layer in the entire frequency range, we used the Drude conductivity model:

$$\varepsilon_g = \varepsilon_\infty - \frac{\omega_p^2}{\omega(\omega + i\gamma)} \quad (1)$$

with fitting values of damping γ and plasma frequency ω_p. Figure 1 shows the calculated spectra, for which we used $\varepsilon_\infty = 1$. The green dashed line in Fig. 1b corresponds to fully coherent plane waves (not shown in Fig. 1a), and the green dotted line was obtained in simulations by neglecting the interference effects, i.e., assuming that the coherence length of the light wave is less than the thickness of the diamond plate. The blue dashed lines in Fig. 1 are the calculation of the transmittance without taking into account multiple reflections in the diamond plate. The best agreement between the results of the calculation and the experiment was achieved when the damping value was 2.5×10^4 cm^{-1} (which corresponds to an energy of 3.1 eV or the electron collision frequency of 1.2×10^{14} s^{-1} in the graphitized layer) and a plasma frequency of 2.14×10^4 cm^{-1} ($\hbar\omega_p$ = 2.65 eV). The found collision frequency exceeds by almost two orders of the value of 5×10^{12} s^{-1} for highly oriented pyrolytic graphite [26], which can be explained by the appearance of a significant number of boundaries between graphite nanocrystallites produced by laser irradiation.

A comparison of the experimental transmittance spectrum obtained with an 'Epsilon' spectrometer in the low-frequency region with the calculated spectrum for fully coherent plane waves demonstrates their good agreement. The oscillations observed in this case arise as a result of multiple reflections from the boundaries of the plane-parallel transparent diamond substrate. In measuring the transmittance with a Fourier spectrometer, the oscillation amplitude decreases, which is, apparently, explained by a decrease in the degree of radiation coherence.

At the high-frequency edge of the measurement range, in the region of 1000–4000 cm^{-1}, good agreement was obtained between the experimental data and the simulation results (Fig. 1a), but a discrepancy arises in the region of optical frequencies: The calculated transmittance is much lower than that in the experiment. However, if $\varepsilon_\infty = 2$ is used in the Drude formula, and the remaining parameters are left unchanged, then a better quantitative agreement between the calculated transmittance and the transmittance in the optical frequency range can be achieved (Fig. 2a). At the same time, good agreement between the calculated and experimental data is preserved in the remaining frequency ranges (see, for example, the low-frequency region in Fig. 2b). The difference in the background permittivity ε_∞ for graphitised diamond from unity in the Drude formula can be explained by the presence of a transient damaged layer of diamond during laser surface graphitisation, which contributes to the effective high-frequency polarisation of the graphitised material. According to Pimenov et al. [20], the optical transmission of diamond irradiated with a laser was not restored to the initial value (~70%) in the case of thermal annealing (at a temperature $T = 560$ °C for 30 min), while measurements using Raman spectroscopy did not detect the

presence of graphitised material. Another argument in favour of this approximation is insufficiently close-to-metallic conductivity of the produced layer, which is confirmed by the proximity of the values of γ and ω_p. Therefore, the use of the permittivity $\varepsilon_\infty = 2$ in the Drude formula can be considered justified.

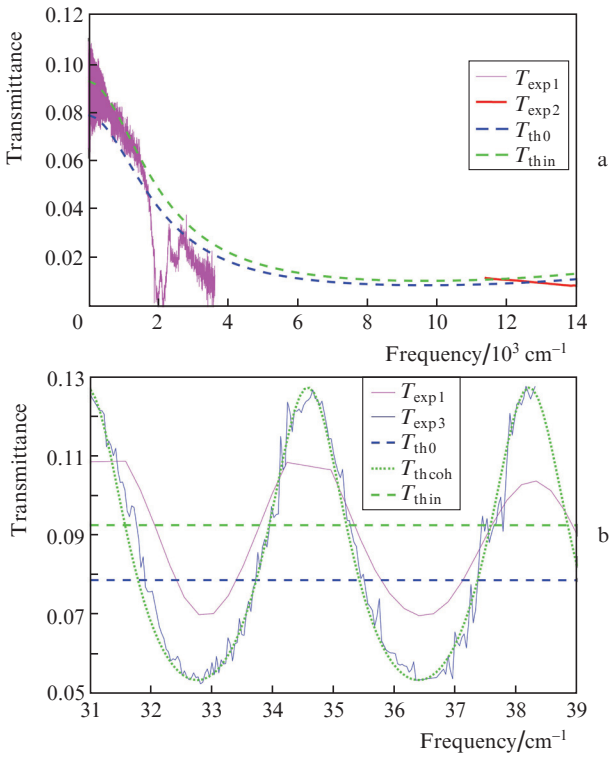

Figure 2. (Colour online) Experimental (solid curves) and calculated (dashed and dotted curves) transmittance spectra of a graphitised layer with $\varepsilon_\infty = 2$ (a) in a wide frequency range and (b) at a low frequency edge. The green dashed line in Fig. 2b corresponds to fully coherent plane waves, green dotted curves were obtained in simulations neglecting interference effects, and blue dashed lines were obtained without taking into account multiple reflections in the diamond plate.

It should be noted that the condition $\omega \ll \gamma$ (Hagen–Rubens regime) is satisfied in the entire range of the analysed frequencies shown in Figs 1 and 2, and this allows the $n_g \approx \kappa_g$ approximation to be used, where $n_g + i\kappa_g \equiv \varepsilon_g^{1/2}$ is refraction index of the graphitised layer. Figure 3 shows the results of modelling the dispersion dependences of n_g and κ_g, performed on the basis of an approximation of the experimental transmission spectra, in comparison with the data for pyrolytic graphite (n_{pg} and κ_{pg}) measured in [27]. One can see that our calculated values are lower than those obtained earlier in [27]; this is apparently explained by worse metal properties (lower conductivity) of graphitised diamond as compared to pyrolytic graphite.

4. Conclusions

Optical transmission spectra of the initial diamond substrate and the plate with a laser-modified surface layer were measured in the range from far-IR to visible. Analysis of the optical properties of the graphitised layer using the Drude conductivity model allowed us to develop a theoretical model

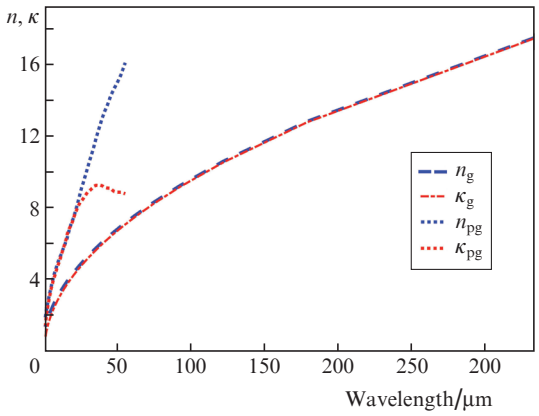

Figure 3. (Colour online) Dispersion dependences of the real (n_g; blue dashed curve) and imaginary (κ_g; red dash-and-dot curve) parts of the calculated refractive index of the graphitised layer and data for pyrolytic graphite (n_{pg}, κ_{pg}; blue and red dotted curves) from [27].

describing the electromagnetic response of surface structures obtained using laser radiation. Based on this model, we calculated optical constants, which make it possible to optimise the optical properties of the fabricated structures in a wide frequency range.

Acknowledgements. The experimental part was supported by the Russian Foundation for Basic Research (Grant No. 16-32-60179 mol_a_dk). The transmission spectra were simulated with the support of the Russian Science Foundation (Grant No. 14-12-01372). The work of M.S. Komlenok and V.I. Konov was supported by the NRNU 'MEPhI' Competitiveness Enhancement Programme.

References

1. Konov V.I. *Laser Photonics Rev.*, **6** (6), 739 (2012).
2. Konov V.I. *Quantum Electron.*, **45** (11), 1043 (2015) [*Kvantovaya Elektron.*, **45** (11), 1043 (2015)].
3. Mildren R., Rabeau J. *Optical Engineering of Diamond* (Weinheim: John Wiley & Sons, 2013).
4. Riedrich-Möller J., Kipfstuhl L., Hepp C., Neu E., Pauly C., Mucklich F., Baur A., Wandt M., Wolff S., Fischer M., Gsell S., Schreck M., Becher C. *Nat. Nanotechnol.*, **7** (1), 69 (2012).
5. Lagomarsino S., Bellini M., Corsi C., Fanetti S., Gorelli F., Liontos I., Parrini G., Santoro M., Sciortino S. *Diamond Relat. Mater.*, **43**, 23 (2014).
6. Oh A., Caylar B., Pomorski M., Wengler T. *Diamond Relat. Mater.*, **38**, 9 (2013).
7. Komlenok M.S., Dezhkina M.A., Kononenko V.V., Khomich A.A., Popovich A.F., Konov V.I. *Bull. Lebedev Phys. Inst.*, **44** (2), 246 (2017) [*Kr. Soobshch. Fiz. FIAN*, (8), 47 (2017)].
8. Kononenko V.V., Gololobov V.M., Konov V.I. *Appl. Phys. A*, **122** (3), 1 (2016).
9. Kononenko T.V., Zavedeev E.V. *Quantum Electron.*, **46** (3), 229 (2016) [*Kvantovaya Elektron.*, **46** (3), 229 (2016)].
10. Simmonds R.D., Salter P.S., Jesacher A., Booth M.J. *Opt. Express*, **19** (24), 24122 (2011).
11. Shimizu M., Shimotsuma Y., Sakakura M., Yuasa T., Homma H., Minowa Y., Tanaka K., Miura K., Hirao K. *Opt. Express*, **17** (1), 46 (2009).
12. Kononenko T.V., Dyachenko P.N., Konov V.I. *Opt. Lett.*, **39** (24), 6962 (2014).
13. Komlenok M.S., Lebedev S.P., Komandin G.A., Piqué A., Konov V.I. *Laser Phys. Lett.*, **15** (3), 036201 (2018).
14. Zaitsev A.M. *Optical Properties of Diamond: a Data Handbook* (Berlin–Heidelberg: Springer Science & Business Media, 2013).

15. Komlenok M.S., Kononenko V.V., Gololobov V.M., Konov V.I. *Quantum Electron*., **46** (2), 125 (2016) [*Kvantovaya Elektron*., **46** (2), 125 (2016)].
16. Komlenok M.S., Dezhkina M.A., Khomich A.A., Orekhov A.S., Ralchenko V.G., Tikhodeev S.G., Konov V.I. *J. Phys.: Conf. Ser*., **1092** (1), 012061 (2018).
17. Komlenok M.S., Tikhodeev S.G., Weiss T., Lebedev S.P., Komandin G.A., Konov V.I. *Appl. Phys. Lett*., **113** (4), 041101 (2018).
18. Kozlov G., Volkov A., in *Millimeter and Submillimeter Wave Spectroscopy of Solids* (Berlin–Heidelberg: Springer, 1998) pp 51–109.
19. Born M., Wolf E. *Principles of Optics* (Oxford: Pergamon Press, 1980; Moscow: Nauka, 1973).
20. Pimenov S.M., Kononenko V.V., Ralchenko V.G., Konov V.I., Gloor S., Lüthy W., Weber H.P., Khomich A.V. *Appl. Phys. A*, **69** (1), 81 (1999).
21. Rehman Z.U., Janulewicz K.A. *Diamond Relat. Mater*., **70**, 194 (2016).
22. Komlenok M.S., Dezhkina M.A., Zavedeev E.V., Khomich A.A., Orekhov A.S., Konov V.I. *Bull. Lebedev Phys. Inst*., **46** (1), 13 (2019) [*Kr. Soobshch. Fiz. FIAN*, (12), 61 (2018)]].
23. Tikhodeev S.G., Yablonskii A.L., Muljarov E.A., Gippius N.A., Ishihara T. *Phys. Rev. B*, **66**, 045102 (2002).
24. Dore P., Nucara A., Cannavò D., De Marzi G., Calvani P., Marcelli A., Sussmann R.S., Whitehead A.J., Dodge C.N., Krehan A.J., Peters H.J. *Appl. Opt*., **37** (24), 5731 (1998).
25. Phillip H.R., Taft E.A. *Phys. Rev*., **136** (5A), A1445 (1964).
26. Philipp H.R. *Phys. Rev. B*, **16** (6), 2896 (1977).
27. Querry M.R., in *Contractor Report* (Kansas City, Missouri University, 1985).